Journal of Hazardous Materials 168 (2009) 304–309

Contents lists available at ScienceDirect

Journal of Hazardous Materials

journal homepage: www.elsevier.com/locate/jhazmat

Removal of Basic Red 46 dye from aqueous solution by adsorption onto Moroccan clay

A. Bennani Karim[a,b], B. Mounir[a,*], M. Hachkar[a], M. Bakasse[c], A. Yaacoubi[b]

[a] The Team of Research Analysis, Checks and Environment, High School of Technology, University Cadi Ayyad, Dar Si Aissa Road, BP 89, Safi, Morocco
[b] The Team Environmental and Experimental Methodology, Laboratory of Organic Applied Chemistry, Faculty of the Sciences Semlalia, BP 2390, Marrakech, Morocco
[c] The Team of Analysis of the Microphones Polluting Organic, Faculty of the Sciences, University Chouaib Doukkali, BP 20, El Jadida, Morocco

ARTICLE INFO

Article history:
Received 31 July 2008
Received in revised form 6 February 2009
Accepted 6 February 2009
Available online 20 February 2009

Keywords:
Basic Red
Moroccan clay
Adsorption
Isotherms
Kinetics
Thermodynamic parameters

ABSTRACT

In this study, Moroccan crude clay of Safi, which was characterized by X-ray diffraction, is used as adsorbent for the investigation of the adsorption kinetics, isotherms and thermodynamic parameters of the Basic Red 46 (BR46) in aqueous solutions at various dye concentrations, adsorbent masses and pH values. The results showed that the adsorption capacity of the dye increased by initial dye concentration and pH values. Two kinetic models (the pseudo-first-order and the pseudo-second-order) were used to calculate the adsorption rate constants. The adsorption kinetics of the basic dye followed pseudo-second-order model. The experimental data isotherms were analyzed using the Langmuir, Freundlich and Dubinin–Radushkevish equations. The monolayer adsorption capacity for BR46 dye is 54 mg/g of crude clay. Nearly 20 min of contact time was found to be sufficient for the dye adsorption to reach equilibrium. Thermodynamical parameters were also evaluated for the dye–adsorbent system and revealed that the adsorption process is exothermic in nature.

© 2009 Elsevier B.V. All rights reserved.

1. Introduction

Dyes are synthetic aromatic compounds which are embodied with various functional groups. They are widely used in textile, leather, paper, plastic, and other industries. Some of these dyes may degrade to produce carcinogens and toxic products [1]. Thus, the removal of dyes from effluents is important for risk assessment.

Several physical or chemical processes are used to treat dye laden wastewaters. These processes include flocculation, precipitation, ion exchange, membrane filtration, electrochemical destruction, irradiation and ozonation. However, these processes are costly and lead to generation of sludge or formation of by-products [2]. Among the physical methods available, adsorption process is one of the most efficient methods to remove dyes from wastewater, especially if the adsorbent is inexpensive and readily available [3]. Activated carbon is the most widely used adsorbent for dye removal, but it is too expensive [4], consequently, numerous low-cost alternative adsorbents have been proposed including: peat [5], sepiolite [6], montmorillonite, chitosan and nanocomposite [7], and pine sawdust [8]. Clays are mostly used as available adsorbent and catalyst [9].

In the present work, adsorption of Basic Red 46 (BR46) dye onto Moroccan crude clay has been investigated and the obtained experimental data were analyzed using adsorption isotherm models namely, Langmuir, Freundlich, and Dubinin–Radushkevich. The effect of pH, adsorbent mass and initial dye concentration has been studied. Kinetic experiments have been also conducted to determine the rate of BR46 adsorption onto clay.

2. Materials and methods

2.1. Materials

The basic dye used as adsorbate in the present study is C.I. Basic Red 46 (Mr = 357.5), which was purchased from SDI textile company (Safi, Morocco). The BR46 molecular structure is shown in Fig. 1. The clay used in this study was ground from the natural basin of Safi and sieved to 0.08–0.1 μm size fraction. Then, it was dried at 105 °C for 24 h and used for further experiments.

The chemical composition of the adsorbent was determined by using Philips X' Cem X-ray fluorescence spectrometer (XRF). The results are given in Table 1. XRD analyses of the powder sample were performed using Siemens D-5000 X-ray diffractometer. The physical properties (including BET, external surface area, total pore volume and micropore volume, as well as average pore size distribution) of crude clay were obtained by measuring their nitrogen adsorption–desorption isotherms at −196 °C with the use of a sur-

* Corresponding author at: Ecole Supérieure de Technologie, Université Cadi Ayyad, BP 89, Safi, Morocco. Tel.: +212 61 28 93 66; fax: +212 24 62 91 24.
E-mail address: mounirbadia@yahoo.fr (B. Mounir).

0304-3894/$ – see front matter © 2009 Elsevier B.V. All rights reserved.
doi:10.1016/j.jhazmat.2009.02.028

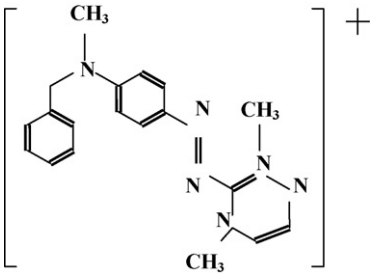

Fig. 1. Molecular structure of BR46.

Table 1
Mineralogical composition of the crude clay.

Element	Percentage (%)
SiO_2	53.11
Al_2O_3	16.95
Fe_2O_3	5.94
CaO	3.51
MgO	2.51
SO_3	0.2
K_2O	4.64
Na_2O	0.26
P_2O_5	0.09

face area and porosity analyser (model no.: ASAP 2010). The results are reported in Table 2. All measurements were repeated twice for the purpose of determining the accuracy of the analytical method.

2.2. Methods

2.2.1. Adsorption experiments

The adsorption experiments were executed in batch. Preliminary experiments demonstrated that the equilibrium was established in 1 h. A 0.04 g sample of clay was mixed with 100 ml dye solution of 20 mg/l in batch. Samples of 3 ml of mixture were withdrawn from the batch at predetermined time intervals and the supernatant was centrifuged for 8 min at 2500 r.p.m. The dye concentrations were determined from their absorbance characteristics in the UV–vis range. A spectrophotometer [GBC (Ajax, Ontorio) UV/visible 911] was used for experiments. A linear correlation was established between the dye concentration and the absorbance at λ_{max} = 530 nm, in the dye concentration range 0–28 mg/l with a correlation coefficient r^2 = 0.99. The adsorption capacity of the dye BR46 was calculated as follows: $q_t = [(C_0 - C_t)V]/W$, where q_t (mg/g) is the amount of BR46 adsorbed at contact time t (min), C_0 (mol/l) is the initial dye concentration, C_t is the dye concentration at time (t), and W (g) is the clay amount in the solution.

Table 2
Surface area and porosity data of the crude clay.

Physical property	Value
Surface area	
Single point surface area at P/P_0 = 0.20044572	42.61 ± 2.02 m^2/g
BET surface area	42.43 ± 2.00 m^2/g
External surface area	42.43 ± 2.42 m^2/g
Pore volume	
Single point adsorption total pore volume of pores less than 351.9365 Å radius at P/P_0 = 0.97191728	0.074556 ± 0.004 cm^3/g
Micropore volume	0.000439 ± 0.00003 cm^3/g
Pore size	
Adsorption average pore radius (2V/A by BET)	3.437 ± 0.2 nm

2.2.2. Effect of adsorbent mass

The effects of varying the clay mass on dye adsorption were carried out by adding 10, 20, 40, 50, and 60 mg samples of clay to 100 ml solution of BR46 aqueous solution having an initial concentration of 20 mg/l.

2.2.3. Effect of initial pH

Effect of initial pH was investigated for various pH values, which are 4, 6, 10.3 and 12. In the experiments, a 0.04 g sample of clay was added to each 100 ml volume of dye aqueous solution having an initial concentration of 20 mg/l. The pH values were adjusted during the experiments by adding a few drops of dilute NaOH or HCl. The point of zero charge (PZC) of the adsorbent was determined using the method described by Ofomaja [10].

2.2.4. Effect of initial dye concentration

The effect of the initial dye concentration was investigated as follows: 0.04 g sample of clay was added to 100 ml solution of BR46 with initial concentrations varying from 10 to 28 mg/l.

2.2.5. Kinetic and adsorption mechanism

The kinetic models of pseudo-first-order, pseudo-second-order were used to examine the adsorption mechanism.

2.2.5.1. Pseudo-first-order model. The pseudo-first-order reaction model [11,12] is described by:

$$\frac{dq_t}{dt} = k_1(q_e - q_t) \quad (1)$$

where q_e and q_t are respectively the amount of dye (mg/g) adsorbed on clay at equilibrium, and at time t, k_1 is the rate constant (min^{-1}). Integrating and applying the boundary conditions (t = 0 and q_t = 0 to t and q_t), Eq. (1) takes the form: $\log(q_e - q_t) = \log q_e - (k_1/2.303)t$. The rate constant k_1 and q_e were obtained from the slope and intercept of the linear plots of $\log(q_e - q_t)$ against t, respectively.

2.2.5.2. Pseudo-second-order model. The pseudo-second-order reaction model [11,12] is expressed by:

$$\frac{dq_t}{dt} = k_2(q_e - q_t)^2 \quad (2)$$

where k_2 is the rate constant of pseudo-second-order sorption (g/(mg min)). Integrating and applying boundary conditions (t = 0 and q_t = 0 to t = t and q_t = q_t), Eq. (2) becomes $q_t = t/[(1/k_2q_e^2) + t/q_e]$ which has linear form of $t/q_t = t/(k_2q_e^2) + (1/q_e)t$. The rate constant k_2 and q_e were obtained from the intercept and slope of the linear plots of t/q_t against t, respectively.

3. Results and discussion

3.1. Characterization of adsorbent

The crude clay composition is presented in Table 1. SiO_2 and Al_2O_3 are the major constituents of the clay with other oxides present in trace amounts. The mineralogical composition of the crude clay was determined from X-ray diffractogram (Fig. 2). The following mineral phases were identified: quartz, illite, kaolinite, dolomite and calcite. The predominant peaks found in the crude clay were 9.99, 7.16, 5.02, 4.47, 4.25, 3.579, 3.34, 3.03 and 2.9 Å which correspond to illite, kaolinite, illite, kaolinite, quartz, kaolinite, quartz + illite, calcite and dolomite. The above data suggest that this clay is a mixed kaolinite–illite clay mineral. In this mixture, the percentages of illite, kaolinite and quartz are respectively 18%, 29% and 32%.

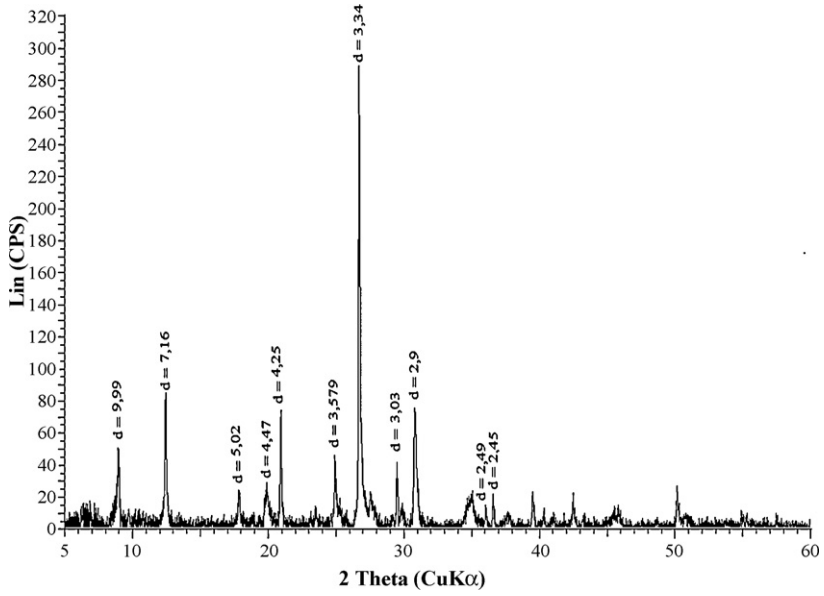

Fig. 2. X-ray diffractometer analysis for the crude clay.

3.2. Effect of adsorbent amount

In order to estimate the optimal amount of crude clay to add to aqueous dye solution, batch experiments were conducted using 100 ml of BR46 solutions at 20 mg/l, adding different amounts of clay (10, 20, 40, 50, and 60 mg) (Fig. 3). It was observed that the uptake of the dye increased by the amount of clay added and that the maximum dye removal was achieved within the amount 40 mg. This implied that the number of adsorption sites increased as adsorbent mass increases (Fig. 3). This can be attributed to the increase in the adsorbent surface area and availability of more adsorption sites. However, the further increase in the amount of the adsorbent did not affect the uptake capacity significantly [13,14]. Such a phenomenon was similar to those of Wen-Tien Tsai for the adsorption of cationic dye onto acid activated andesite [13]. Consequently, 40 mg was used as optimal amount for further experiments.

3.3. Kinetic studies

The time-dependent dye adsorption behaviour was monitored by varying the equilibrium time between adsorbate and adsorbent in the range of 1–60 min. The adsorption capacity of the dye as a function of contact time plotted in Fig. 4 indicates that the equilibrium between the dye and the clay was attained in 20 min. In this study, the initial BR46 concentrations used are 10, 16, 20, 24 and 28 mg/l. The dependence of these concentrations against time is shown in Fig. 4.

Two kinetic models were tested to explain the data presented in Fig. 4: pseudo-first-order, and pseudo-second-order models. The agreement between experimental data and model-calculated values is expressed by the correlation coefficient (r^2). The results are reported in Table 3. The lower values of r^2 and the difference between the experimental and calculated equilibrium sorption show that the pseudo-first-order model failed to describe the adsorption kinetics. The higher values of $r^2 > 0.99$ and the good agreement between the experimental and calculated equilibrium sorption for the pseudo-second-order model confirm that this one describes correctly the adsorption kinetics. The values of the rate constants (k_2) were found to decrease from 0.32 to 0.085 mg/(g min) as the initial concentration increased from 10 to 28 mg/l, showing the process to be highly concentration dependent, which is consistent with earlier studies [11,13].

3.4. Effect of initial dye concentration

Fig. 4 shows the effect of initial dye concentration on the adsorption rate of the dye at pH 6 and 293 K. An increase in initial dye

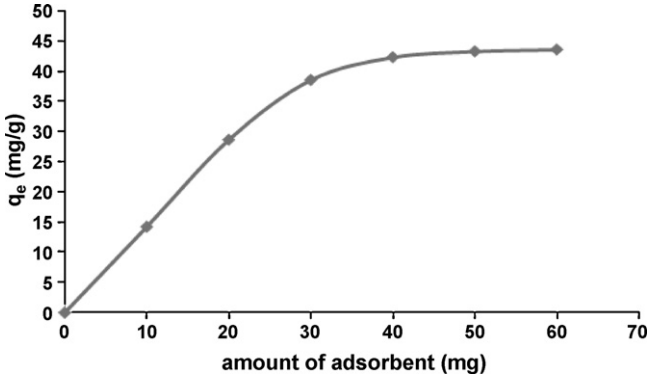

Fig. 3. Plots of equilibrium amount of BR46 adsorbed onto clay versus adsorbent amount at various adsorbent masses (10, 20, 30, 40, 50, and 60 mg) at equilibrium time t_{eq} = 2 h.

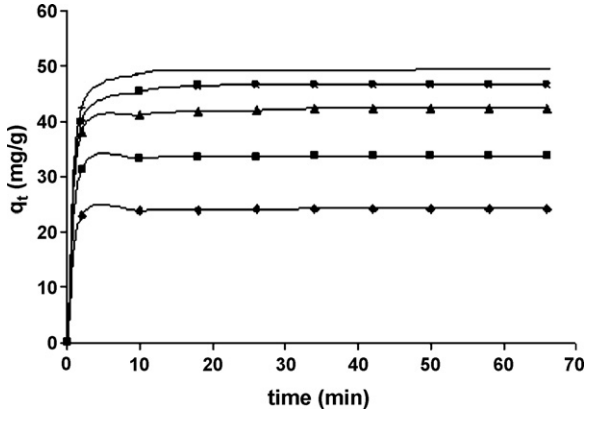

Fig. 4. Kinetic curves of BR46 retention by clay at different initial BR46 concentrations (♦: 10 mg/l; ■: 16 mg/l; ▲: 20 mg/l; ■: 24 mg/l; –: 28 mg/l).

Table 3
Kinetic parameters for the effect of solution concentrations.

Concentration (mg/l)	$q_{e\,exp}$ (mg/g)	Pseudo-first-order kinetic			Pseudo-second-order kinetic		
		q_e (mg/g)	k_1(min^{-1})	r^2	q_e (mg/g)	k_2 (g/(mg min))	r^2
10	24.13	5.29	0.183	0.72	24.21	0.328	0.999
16	33.71	8.14	0.2	0.85	33.78	0.224	0.999
20	42.31	10.26	0.15	0.84	42.55	0.09	0.999
24	46.63	11.06	0.163	0.92	46.94	0.0856	0.999
28	49.39	12.09	0.18	0.92	49.5	0.085	0.999

concentration leads to an increase in the adsorption capacity. As the initial dye concentration increases from 10 to 28 mg/l, the adsorption capacity of dye onto clay changes from 24.13 to 49.31 mg/g (Fig. 4). This indicates that the initial dye concentration plays an important role in the adsorption capacity of dye [11]. Moreover, the initial rate of adsorption was greater for higher initial dye concentration because the resistance to the dye uptake decreased as the mass transfer driving force increased [15]. The time rate adsorption curves (Fig. 4) are single, smooth and continuous leading to saturation at various concentrations of BR46. This shows the possibility of full coverage of the external surface of the clay by BR46 [16].

3.5. Effect of initial pH

The pH is one of the determining parameters of controlling the adsorption behaviour of cationic molecule onto suspended clay particles. The variation of BR46 adsorption onto clay over a pH range 4–12 is shown in Fig. 5. The pH PZC value for the crude clay studied was 9.5. The adsorption capacity of BR46 onto the studied clay increased significantly when the pH of dye solution increased from 9.5 to 12. This means that the charge sign on the surface of the clay remains negative in a wide pH range (9.5–12). When the solution pH is basic, the negative charged clay surface favours the BR46 adsorption. Therefore, the amount of BR46 adsorbed on the clay tended to decrease with the decrease of pH, which can be attributed to the electrostatic repulsion between the positively charged surface and the positively charged dye molecule for pH below 9.5. Also, the lower adsorption of BR46 at acidic pH may be due to the presence of excess H^+ ions competing with dye cations for the adsorption sites. These observations were similar to those findings by other workers [13,17,18].

Table 4
Thermodynamic parameters.

Temperature (K)	k_d	ΔG° (kcal/mol)	ΔH° (kcal/mol)	ΔS° (kcal/mol)
303	17.39	−38.37	–	–
313	16.29	−38.79	−25.60	0.04
323	15.71	−39.21	–	–
333	15.04	−39.63	–	–

3.6. Thermodynamic parameters

A sample of 40 mg of clay was added to dye solution (100 ml and 10 mg/l) at pH 6. The experiments were carried out at 30, 40, 50 and 60 °C in a constant temperature shaker bath which controlled the temperature to within ±1 °C.

The thermodynamic parameters of the adsorption were determined using the following equations: $\ln(k_d) = \Delta S_{ads}/R - \Delta H_{ads}/RT$ and $\Delta G_{ads} = \Delta H_{ads} - T\Delta S_{ads}$, where k_d is the distribution coefficient at different temperatures (303, 313, 323 and 333 K) and is equal to the ratio of the equilibrium amount adsorbed (q_e in mg/g) to the equilibrium concentration (C_e in mg/l) at different temperatures ($k_d = q_e/C_e$) and R is the gas constant. The second equation was applied to calculate the standard Gibbs free energies ΔG_{ads} and the standard entropy ΔS_{ads}. The values of ΔH_{ads} and ΔS_{ads} were obtained from the slope and intercept of the linear plot of $\log k_d$ versus $1/T$, respectively (Fig. 6). The negative values of ΔG_{ads} (Table 4) indicate that the adsorption of Basic Red 46 (BR46) onto clay is spontaneous [19]. The negative value of ΔH_{ads} suggests that the process is exothermic in nature. The positive value of ΔS_{ads} shows increased randomness at the solid–solution interface during the adsorption of dye onto clay [12]. Generally, the value of ΔG_{ads} for physical adsorption is less than −4.7 kcal/mol. The value of ΔG_{ads} for this case is less than −4.7 kcal/mol suggesting that the process is controlled by physical adsorption [20].

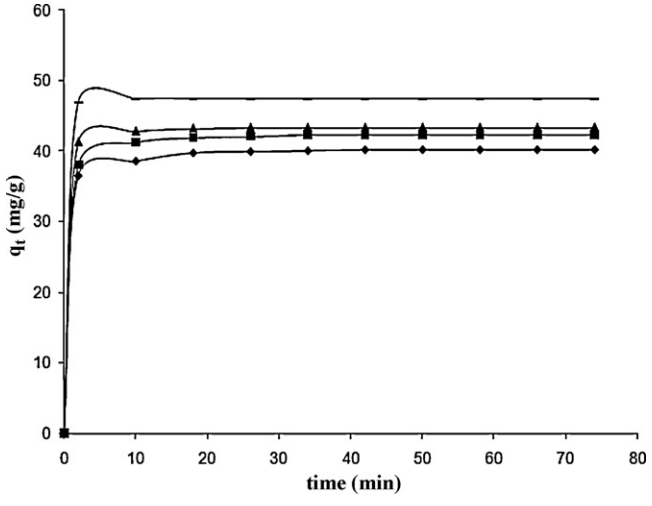

Fig. 5. pH effect on the adsorption of BR46 onto clay (♦: pH 4; ■: pH 6; ▲: pH 10.3; –: pH 12).

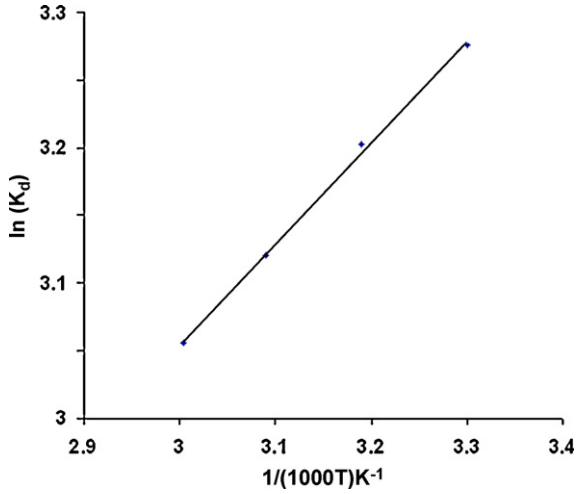

Fig. 6. Van't Hoff plot for the dye adsorption on the clay.

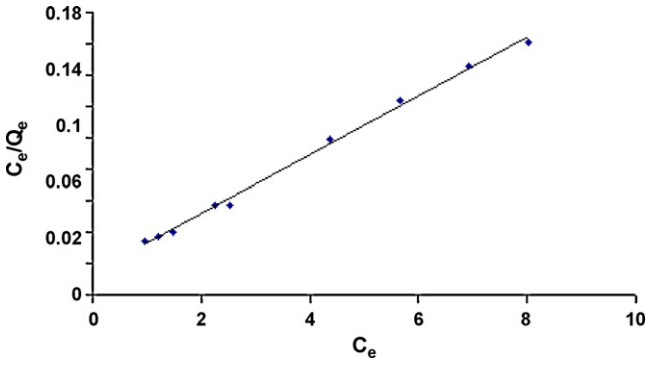

Fig. 7. Langmuir plot for the BR46 adsorption onto clay.

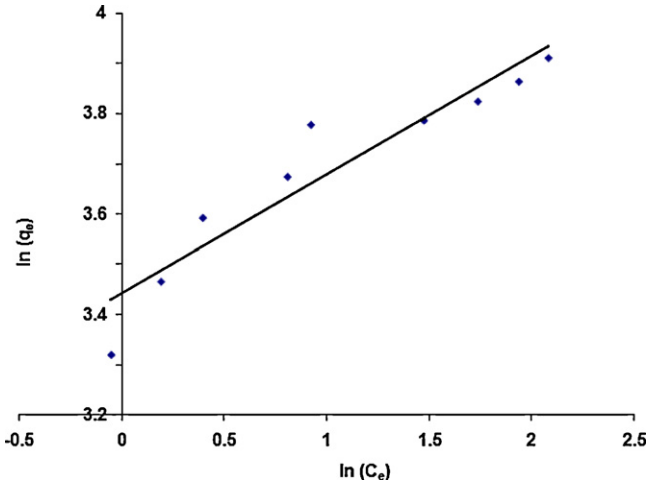

Fig. 8. Freundlich plot for the BR46 adsorption onto clay.

3.7. Equilibrium studies

The equilibrium isotherms are very important for understanding the adsorption systems. The variation of the dye concentration method, while keeping the same mass of the adsorbent, is used to calculate the adsorption characteristics of the adsorbent. The adsorption isotherms used to describe the BR46-clay (liquid–solid) adsorption system are Langmuir, Freundlich and Dubinin–Radushkuvich isotherms.

3.7.1. Langmuir isotherm

The equilibrium data for BR46 dye over the concentration range from 10 to 28 mg/l at 25 °C were fit to the Langmuir isotherm. The following relation can represent the linear form of the Langmuir isotherm model: $C_e/q_e = 1/(q_{max}K_a) + C_e/q_{max}$, where q_e is the amount adsorbed at equilibrium (mg/g), C_e the equilibrium concentration of the adsorbate (mg/l), q_{max} (mg/g) and K_a (l/mg) are the Langmuir constants related to the maximum adsorption capacity and the energy of adsorption, respectively. These constants can be evaluated from the intercept and the slope of the linear plot of experimental data of C_e/q_e versus C_e, respectively (Fig. 7). As seen in Table 5, the Langmuir maximum capacity was found to be 54 mg/g. The Langmuir isotherm has generated a satisfactory fit to the experimental data as indicated by correlation coefficient. This may be due to homogeneous distribution of active sites on the clay surface, since the Langmuir equation assumes that the surface is homogeneous [8]. The monolayer formation for the present system has been confirmed by the linear plot (Fig. 7). Similar observations were reported for the adsorption of direct dye on palm ash [21], removal of Rhodamine B onto sodium montmorillonite [18] and also for the adsorption of basic dye onto sepiolite [15].

The essential feature of the Langmuir isotherm can be expressed by means of a dimensionless constant separation factor or equilibrium parameter R_L, which is defined by the relationship $R_L = 1/(1 + K_L C_0)$, where C_0 is initial concentration (mg/l), and K_L is the Langmuir constant (l/mg). The R_L value calculated is 0.24 (Table 5) which is between 0 and 1 indicating that the adsorption of BR46 onto clay is favourable [21].

Table 5
Langmuir, Freundlich and Dubinin–Radushkuvich parameters.

Crude clay	
Langmuir isotherm	
q_{max} (mg/g)	54
K_L (l/mg)	1.248
R_L	0.24
r_L^2	0.99
Freundlich isotherm	
K_F (mg/g)	31.22
$1/n$	0.23
r_F^2	0.89
Dubinin–Radushkuvich isotherm	
q_{max} (mg/g)	47.99
E (kJ/mol)	10.2
B_D (mol^2 kJ^{-2})	0.0018
r_D^2	0.97

3.7.2. Freundlich isotherm

The performance of the clay in dye removal from the aqueous solution has also been studied using the Freundlich isotherms. The following relation represents the linear form of Freundlich isotherm model: $\log q_e = (1/n)\log C_e + \log K_F$; $1/n$ is the adsorption intensity, K_F represents the adsorption capacity related to Freundlich isotherm. These constants can be evaluated from the intercept and the slope of the linear plot of $\log q_e$ versus $\log C_e$ (Fig. 8). The slope $1/n$, ranging between 0 and 1 (Table 5) is indicative of the relative energy distribution on the adsorbent surface (or surface heterogeneity) [22]. The Langmuir correlation coefficient r_L^2 is higher than the Freundlich correlation coefficient r_F^2. It indicates that the Langmuir isotherm shows better fit to adsorption than the Freundlich isotherm. Similar observations were reported for equilibrium studies of the acid dye adsorption onto modified hectorite [23].

3.7.3. Dubinin–Radushkevich isotherm

The mechanism of BR46 adsorption from solution onto clay surface was then examined with the Dubinin–Radushkevich (D–R) equation: $q_e = q_{max}\exp(-B_D\ [RT\ln(1 + 1/C_e)]^2)$, where q_e is the amount of BR46 adsorption in (mg/g), q_{max} (mg/g) is the D–R monolayer capacity, T (°K) is the temperature and C_e is the equilibrium concentration of BR46 at solution. The adsorption data were analyzed using the linear form of the D–R isotherm for the crude clay: $\ln q_e = \ln q_{max} - B_D\varepsilon^2$, where q_e is the amount adsorbed at equilibrium (mg/g), q_{max} (mg/g) is the Moroccan clay monolayer capacity, B_D (mol^2 kJ^{-2}) is a constant related to sorption energy, and ε is the Polanyi potential, which is related to the equilibrium concentration as $\varepsilon = RT\ln(1 + 1/C_e)$. The plot of specific sorption, $\ln q_e$, against ε^2 for BR46 is shown in Fig. 9. The isotherm constants are presented in Table 5. The slope and intercept of the plots of $\ln q_e$ versus ε^2 give B_D and q_{max}, respectively. The value of B_D is related to sorption energy E, via the following relationship $E = 1/(2B_D)^{0.5}$. The mean adsorption energy is the free energy change when 1 mol of the ion is transferred to the surface of the solid from infinity in the solution [17]. Its value in the range of 8–16 kJ mol^{-1} indicates physical adsorption [24], while its value in the range of 20–40 kJ mol^{-1} is indicative of chemisorption [17]. The value of E (10.91 kJ/mol) in the present case

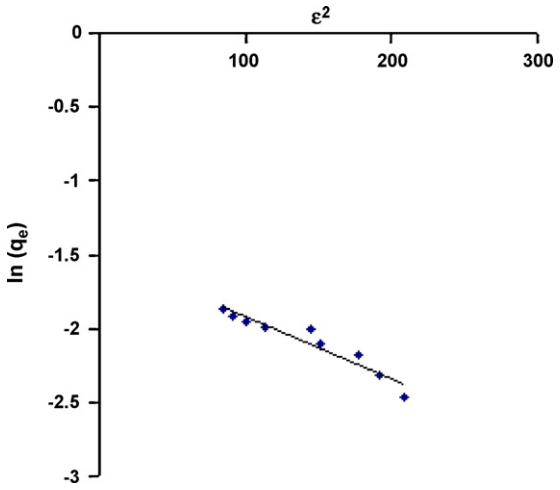

Fig. 9. Dubinin–Radushkuvich plot for the BR46 adsorption onto clay.

is found to be between 8 and 16 kJ/mol (Table 5) corresponding to physical adsorption.

4. Conclusion

Equilibrium and kinetic studies were performed for the adsorption of BR46, a cationic dye, from its aqueous solutions by Moroccan crude clay. The results showed that the adsorption may reach 95% of the total adsorption capacity in 20 min. Adsorption was found to be spontaneous and exothermic in nature. The equilibrium data have been analyzed against Freundlich, Langmuir, and Dubinin–Radushkevich models. The characteristic parameters for each isotherm have been determined. The obtained results showed that the adsorption equilibrium data fitted well to three models and the Langmuir isotherm shows a better fit to adsorption than the Freundlich isotherm. The maximum removal capacity for the BR46 by the used clay is 54 mg/g. The adsorption was rapid and pH, initial dye concentration, adsorbent mass dependent. Also, evaluation of the adsorption results obtained on the basis of different kinetic models showed that dye/clay system was best described by the pseudo-second-order model.

References

[1] M. Teng, S. Lin, Removal of basic dye from water onto pristine and HCl-activated montmorillonite in fixed beds, Desalination 194 (2006) 156–165.
[2] T. Robinson, G. McMullan, R. Marchant, P. Nigam, Remediation of dyes in textile effluent: a critical review on current treatment technologies with a proposed alternative, Bioresour. Technol. 77 (2001) 247–255.
[3] A. Al-Futaisi, A. Jamrah, R. Al-Hanai, Aspects of cationic dye molecule adsorption to palygorskite, Desalination 214 (2007) 327–342.
[4] P.K. Malik, Use of activated carbons prepared from sawdust and rice-husk for adsorption of acid dyes: a case study of acid yellow 36, Dyes Pigments 56 (2003) 239–249.
[5] K.R. Ramakrishna, T. Viraraghavan, Dye removal using low cost adsorbents, Water Sci. Technol. 36 (1997) 189–196.
[6] E. Eren, B. Afsin, Investigation of a basic dye adsorption from aqueous solution onto raw and pre-treated sepiolite surfaces, Dyes Pigments 73 (2007) 162–167.
[7] L. Wang, A. Wang, Adsorption characteristics of congo red onto the chitosan/montmorillonite nanocomposite, J. Hazard. Mater. 147 (2007) 979–985.
[8] M. Ozacar, I.A. Sengil, Adsorption of metal complex dyes from aqueous solutions by pine sawdust, Bioresour. Technol. 96 (2005) 791–795.
[9] M. Roulia, A.A. Vassiliadis, Interactions between C.I. Basic Blue 41 and aluminosilicate sorbents, J. Colloid Interf. Sci. 291 (2005) 37–44.
[10] A.E. Ofomaja, Kinetics and mechanism of methylene blue sorption onto palm kernel fibre, Process Biochem. 42 (2007) 16–24.
[11] A. Gürses, Ç. Dogar, M. Yalçin, M. Açikyildiz, R. Bayrak, S. Karaca, The adsorption kinetics of the cationic dye, methylene blue, onto clay, J. Hazard. Mater. B131 (2006) 217–228.
[12] Y. Önal, C. Akmil-Basar, Ç. Sarici-Özdemir, Investigation kinetics mechanisms of adsorption malachite green onto activated carbon, J. Hazard. Mater. 146 (2007) 194–203.
[13] W.T. Tsai, H.C. Hsu, T. Yi Su, K. Yu Lin, C. Ming Lin, T.H. Dai, The adsorption of cationic dye from aqueous solution onto acid-activated andesite, J. Hazard. Mater. 147 (2007) 1056–1062.
[14] V.K. Gupta, A. Mittal, V. Gajbe, Adsorption and desorption studies of water soluble dye, Quinoline Yellow, using waste materiels, J. Colloid Interf. Sci. 284 (2005) 89–98.
[15] B. Karagozoglu, M. Tasdemir, E. Demirbas, M. Kobya, The adsorption of basic dye (Astrazon Lue FGRL) from aqueous solutions onto sepiolite, fly ash and apricot shell activated carbon: kinetic and equilibrium studies, J. Hazard. Mater. 147 (2007) 297–306.
[16] M. Doğan, M. Alkan, A. Türkyilmaz, Y. Özdemir, Kinetics and mechanism of removal of methylene blue by adsorption onto perlite, J. Hazard. Mater. B 109 (2004) 141–148.
[17] S.S. Tahir, N. Rauf, Removal of cationic dye from aqueous solutions by adsorption onto bentonite clay, Chemosphere 63 (2006) 1842–1848.
[18] P. Panneer Selvam, S. Preethi, P. Basakaralingam, N. Thinakaran, A. Sivasamy, S. Sivanesan, Removal of Rhodamine B from aqueous solution by adsorption onto sodium montmorillonite, J. Hazard. Mater. 155 (2008) 39–44.
[19] M.K. Purkait, S. DasGupta, S. De, Adsorption of eosin dye on activated carbon and its surfactant based desorption, J. Environ. Manage. 76 (2005) 135–142.
[20] C.H. Weng, Y.F. Pan, Adsorption of a cationic dye (methylene blue) onto spent activated clay, J. Hazard. Mater. 144 (2007) 355–362.
[21] A.A. Ahmad, B.H. Hameed, N. Aziz, Adsorption of direct dye on palm ash: kinetic and equilibrium modeling, J. Hazard. Mater. 141 (2007) 70–76.
[22] W.T. Tsai, Y.M. Chang, C.W. Lai, C.C. Lo, Adsorption of basic dyes in aqueous solution by clay adsorbent from regenerated bleaching earth, Appl. Clay Sci. 29 (2005) 149–154.
[23] P. Baskaralingam, M. Pulikesi, V. Ramamurthi, S. Sivanesan, Equilibrium studies for the adsorption of acid dye onto modified hectorite, J. Hazard. Mater. B 136 (2006) 989–992.
[24] A. Benhammou, A. Yaacoubi, L. Nibou, B. Tanouti, Adsorption of metal ions onto Moroccan stevensite: kinetic and isotherm studies, J. Colloid Interf. Sci. 282 (2005) 320–326.